Supporting Information

Lighting up Si nanoparticle arrays by exploiting the bound states in the continuum formed in a Si/Au hybrid nanostructure

*Lidan Zhou [1, 2#], Mingcheng Panmai[1#], Shulei Li[1, 3], Yuheng Mao[1], Weichen He[1], Hongxin Huang[1] and Sheng Lan[1]**

[1]Guangdong Provincial Key Laboratory of Nanophotonic Functional Materials and Devices, School of Information and Optoelectronic Science and Engineering, South China Normal University, Guangzhou 510006, China.

[2]State Key Laboratory of Optoelectronic Materials and Technologies, School of Electronics and Information Technology, Sun Yat-sen University, Guangzhou 51006, China.

[3]School of Optoelectronic Engineering, Guangdong Polytechnic Normal University, Guangzhou 510665, China

[#] These authors contributed equally to this work.

*Corresponding author: Sheng Lan; slan@scnu.edu.cn

Table of contents

Supplementary Note 1: Morphology characterization of fabricated Si nanopillars

The morphologies of the fabricated Si nanopillars, including regular arrays of isolated and coupled Si nanopillars, were examined by using scanning electron microscopy (SEM). In Figure S1, we show the SEM images for regular arrays of Si nanopillars with a large (p = 5.0 μm) and a small (p = 320 nm) pitch, including different magnifications and view angles (top view and incline view). It can be seen that Si nanopillars with uniform sizes and well-defined periods were successfully fabricated by using the combination of electron beam lithography and reactive ion etching.

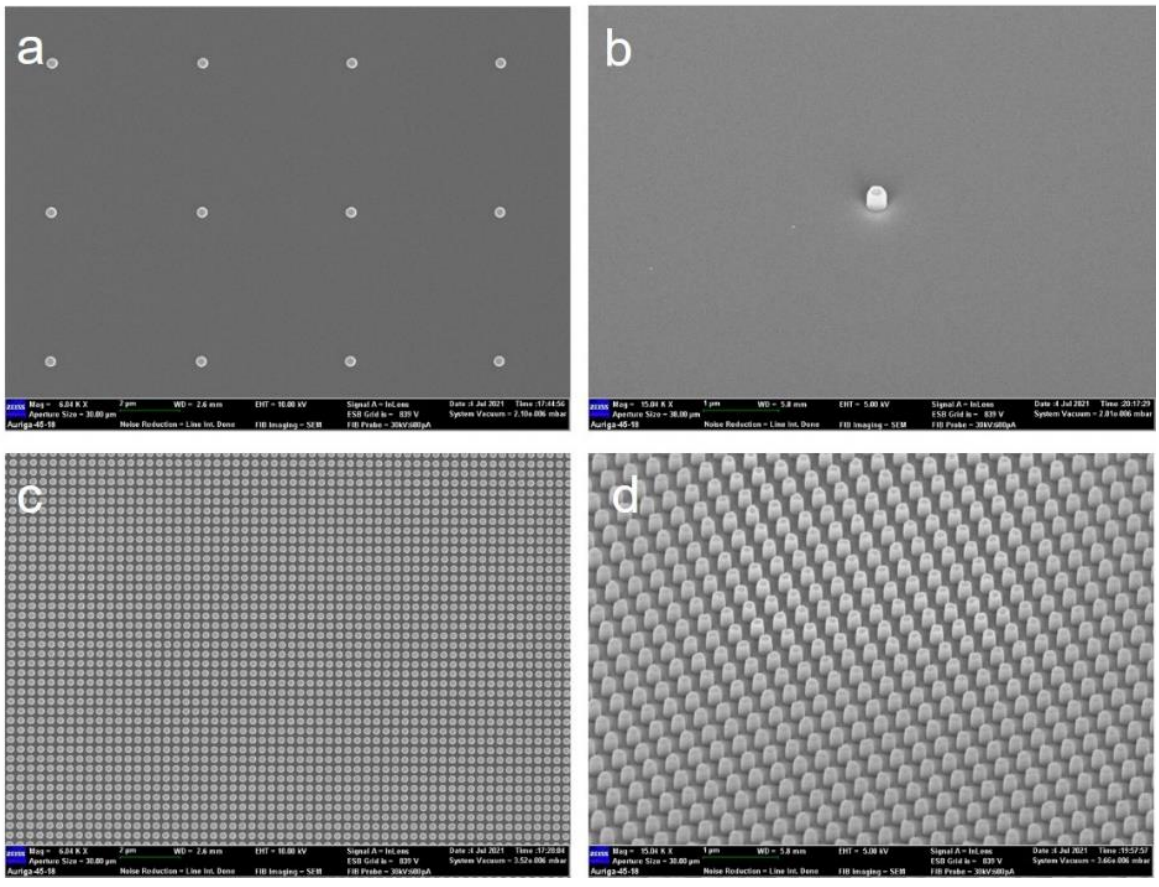

Figure S1. (a) SEM image (top view) of a regular array of isolated Si nanopillars with a pitch of p = 5.0 μm fabricated on an Au/SiO_2 substrate. The diameter of Si nanopillar is d = 260 nm. (b)

SEM image (incline view) of a single Si nanopillar on the Au/SiO_2 substrate with a diameter of d = 260 nm. (c) SEM image (top view) of a regular array of coupled Si nanopillars with a pitch of p = 320 nm fabricated on an Au/SiO_2 substrate. The diameter of Si nanopillar is d = 190 nm. (d) SEM image (incline view) of the regular array of coupled Si nanopillars on the Au/SiO_2 substrate with a pitch of p = 320 nm and a diameter of d = 190 nm.

Supplementary Note 2: Multipolar expansion analysis for the backward scattering spectra of Si nanopillars

In a Cartesian coordinate, the multipolar expansion of ED, MD, EQ, and MQ can be expressed as follows:[1-3]

$$\mathrm{ED} = \frac{1}{-i\omega}\int \mathrm{j} d^3r \tag{1a}$$

$$\mathrm{MD} = \frac{1}{2c} = \int (\mathrm{r}\times\mathrm{j}) d^3r \tag{1b}$$

$$\mathrm{EQ}_{\alpha\beta} = \frac{1}{-i2\omega} = \int\left[r_\alpha j_\beta + r_\beta j_\alpha - \frac{2}{3}(r\cdot j)\delta_{\alpha\beta}\right] d^3r \tag{1c}$$

$$\mathrm{MQ}_{\alpha\beta} = \frac{1}{3c}\int\left[(\mathrm{r}\times\mathrm{j})_\alpha r_\beta + (\mathrm{r}\times\mathrm{j})_\beta r_\alpha \right] d^3r \tag{1d}$$

Here, c is the speed of light in vacuum, α and β represent the Cartesian coordinate components x, y, and z. In Eq. (1), the current density is given by:

$$\mathrm{J}(\mathrm{r}) = -i\omega\varepsilon_0\left[\varepsilon_\mathrm{r}(\mathrm{r}) - \varepsilon_{\mathrm{r,d}}\right]\mathrm{E}(\mathrm{r}) \tag{2}$$

The radiated power of the multipolar moments was calculated as follows:

$$I = \frac{2\omega^4}{3c^3}|ED|^2 + \frac{2\omega^4}{3c^3}|MD|^2 + \frac{\omega^6}{5c^5}\sum|EQ_{\alpha\beta}|^2 + \frac{\omega^6}{40c^5}\sum|MQ_{\alpha\beta}|^2 + O\left(\frac{1}{c^5}\right) \tag{3}$$

In Figure S2, we show the multipolar expansion of the scattering spectrum calculated for a Si nanopillar (h = 220 nm, d = 260 nm,) on a SiO_2/Au/Si substrate.

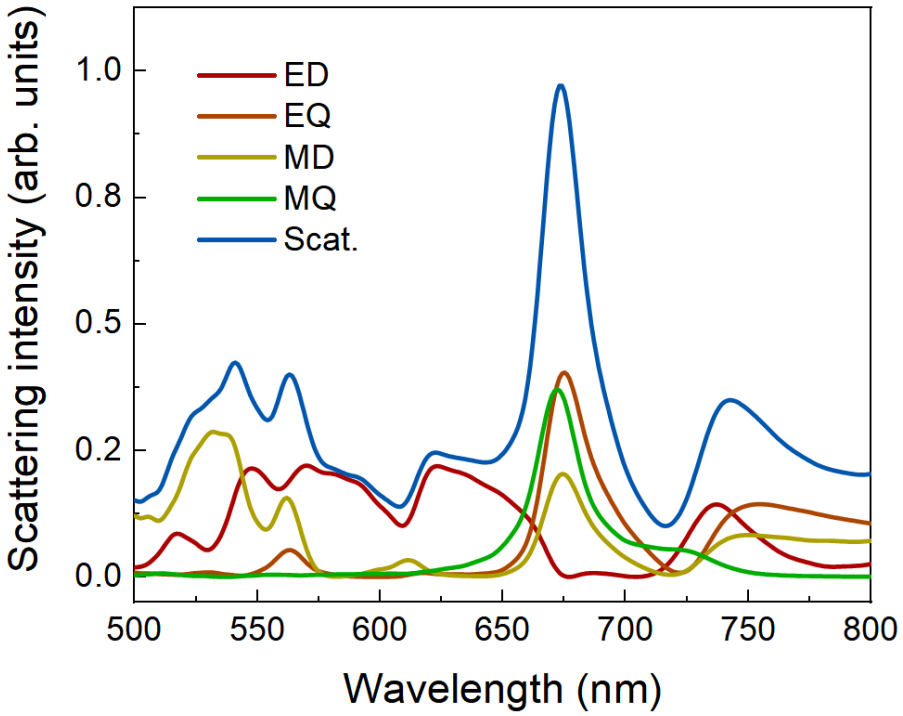

Figure S2. Multipolar expansion of the scattering spectrum of a Si nanopillar (h = 220 nm, d = 260 nm) on a SiO_2/Au/Si substrate. The thicknesses of the SiO_2 spacer layer and the thin Al_2O_3 passivation layer are set to be t_{SiO2} = 10 nm and t_{Al2O3}= 5 nm.

Supplementary Note 3: Determination of bound states in the continuum

In order to find out the influences of the diameter and period of Si nanopillars on the formation of bound states in the continuum (BIC), we calculated the two-dimensional reflection spectra for regular arrays of Si nanopillars with different diameters and periods of Si nanopillars, as shown in Figure S3a–d. In each case, one can see the formation of BIC when the period of the regular array is appropriately chosen, as enclosed by the dashed circle. With increasing the diameter of Si nanopillars, however, a redshift of the BIC is observed. In Figure S3e–i, we present the reflection spectra calculated for the regular array of Si nanopillars with d = 200 nm at different lattice constants (periods). It is noticed that the reflection dip almost disappears for p = 335 nm, implying the formation of a BIC.

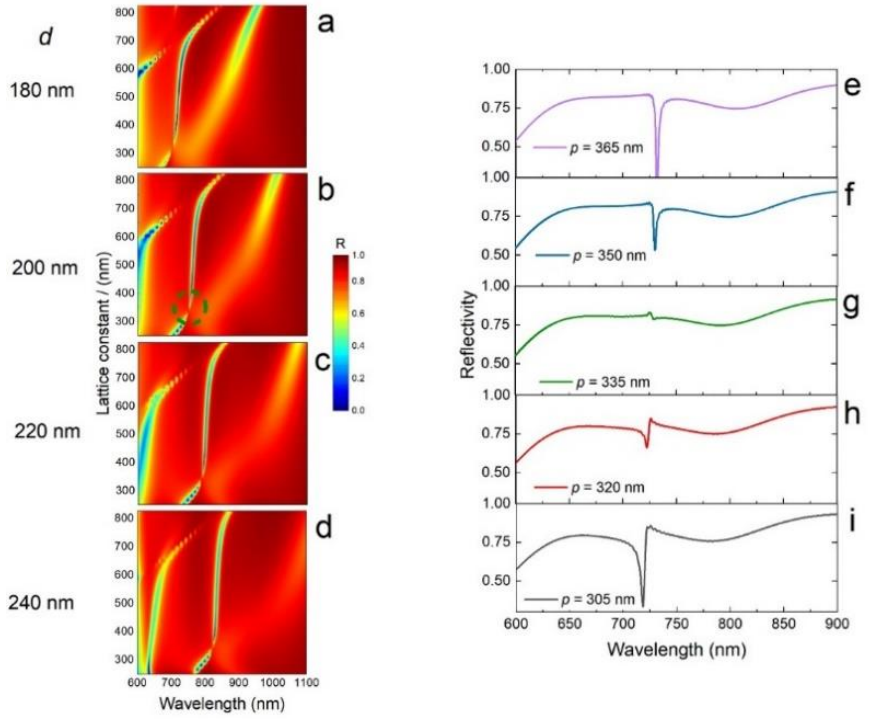

Figure S3. (a–d) Two-dimensional reflection spectra calculated for the regular arrays of Si nanopillars with different diameters on an Au/SiO_2 substrate. The point where the BIC appears is

enclosed by the dashed circle. The reflection spectra for the regular arrays of Si nanopillars with periods around the BIC point are presented in (e–i).

Supplementary Note 4: Analysis of Friedrich-Wintgen BIC based on the temporal coupled-mode theory

In order to gain a deep insight into the formation of the Friedrich-Wintgen BIC (FW-BIC) in the Si/Au hybrid nanostructure, we present a theoretical analysis for the interaction of the SPP and MMD modes supported by the Si/Au hybrid nanostructure based on the temporal coupled-mode theory (see the details in the main text). In Figure 3a, the SPP and MMD modes are marked by grey and white lines. The FW-BIC is formed in the lower hybrid state adjacent to the anti-crossing point of two modes. As shown in Figure S4a, the phase difference between the two modes is close to 0 at the BIC point. In Figure S4b, we show the reflection spectrum obtained at an incident angle of $\theta = 50°$ where the two modes are decoupled. The decay rates of the two modes, which are reflected in the linewidths of the two resonances in the reflection spectrum, are estimated to be $\gamma_{SPP} = 0.068$ meV and $\gamma_{MMD} = 0.032$ meV. These parameters are used in the fitting of the angle-resolved reflection spectra, from which the two hybrid states are extracted (see the solid curves in Figure 3a).

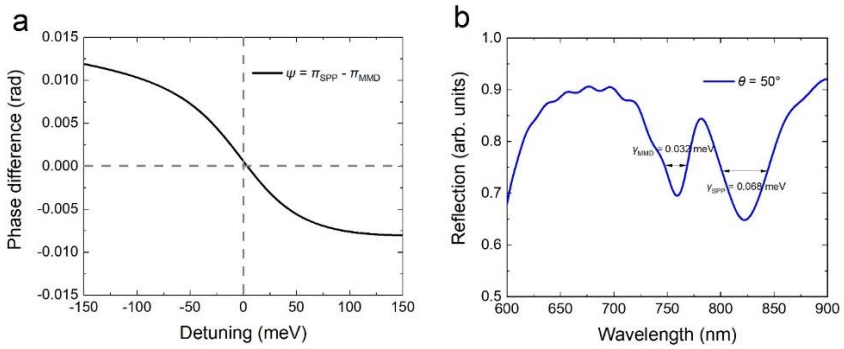

Figure S4. (a) Phase difference as a function of detuning calculated for the SPP and MMD modes supported by the Si/Au hybrid nanostructure (h = 220 nm, d = 190 nm, p = 320 nm). (b) Reflection spectrum of the Si/Au hybrid nanostructure obtained at an incident angle of $\theta = 50°$.

Supplementary Note 5: Reflection spectra calculated and measured for regular arrays of Si nanopillars

Basically, the FW-BIC supported by the regular array of Si nanopillars originates from the interference of the MMD and SPP modes. While the MMD mode is almost independent on the incident angle of the excitation light, the SPP mode is shifted to a longer wavelength with increasing incident angle (or equivalently the period of the regular array). As a result, the intersection of the two optical modes is expected at a certain incident angle where the BIC is formed. In Figure S5, we present a comparison between the simulated angle-resolved reflection spectra and the measured noes for regular arrays of Si nanopillars with different periods. It is found that the experimental observations are in good agreement with the simulation results.

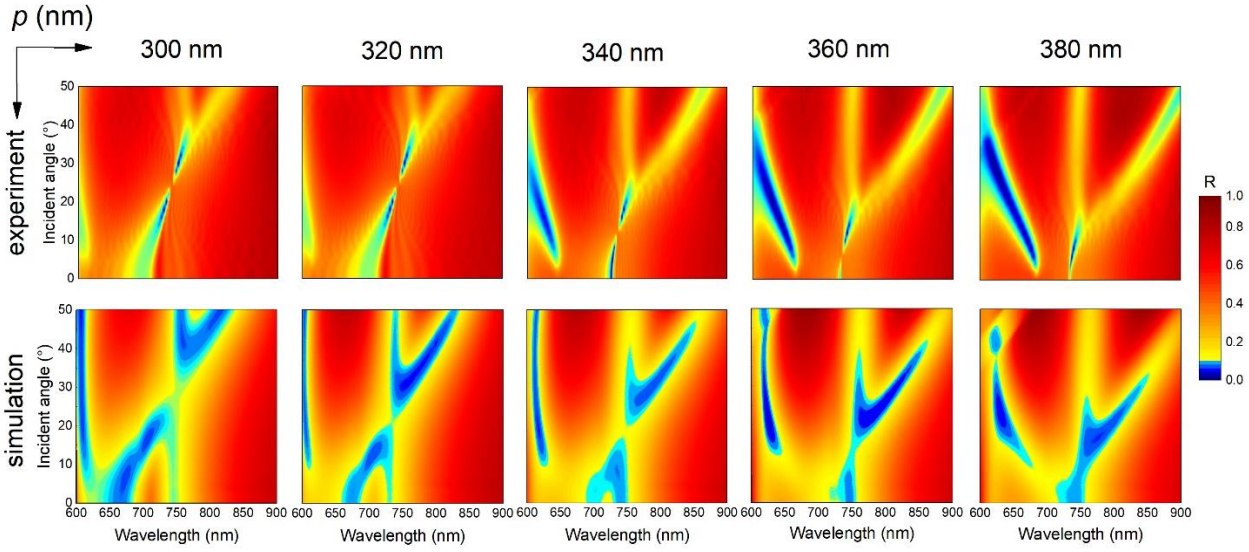

Figure S5. Reflection spectra calculated and measured for regular arrays of Si nanopillars. Angle-resolved reflection spectra measured (upper panel) and simulated (lower panel) for regular arrays of Si nanopillars with different lattice constants (or periods).

Supplementary Note 6: Reflection spectra of the regular array of Si nanopillars excited by using p- and s-polarized light

We examined the angle-resolved reflection spectra of a regular array of Si nanopillars excited by using *p*- and *s*-polarized white light, as shown in Figure S6. It was found that an anti-crossing behavior is observed at ~740 nm when p-polarized white light was employed. In this case, a FW-BIC was created at ~740 nm when the incident angle was chosen to be 22 °. In contrast, no SPP was excited and the MMD remained unchanged with increasing incident angle when s-polarized white light was used. No BIC was created in this case.

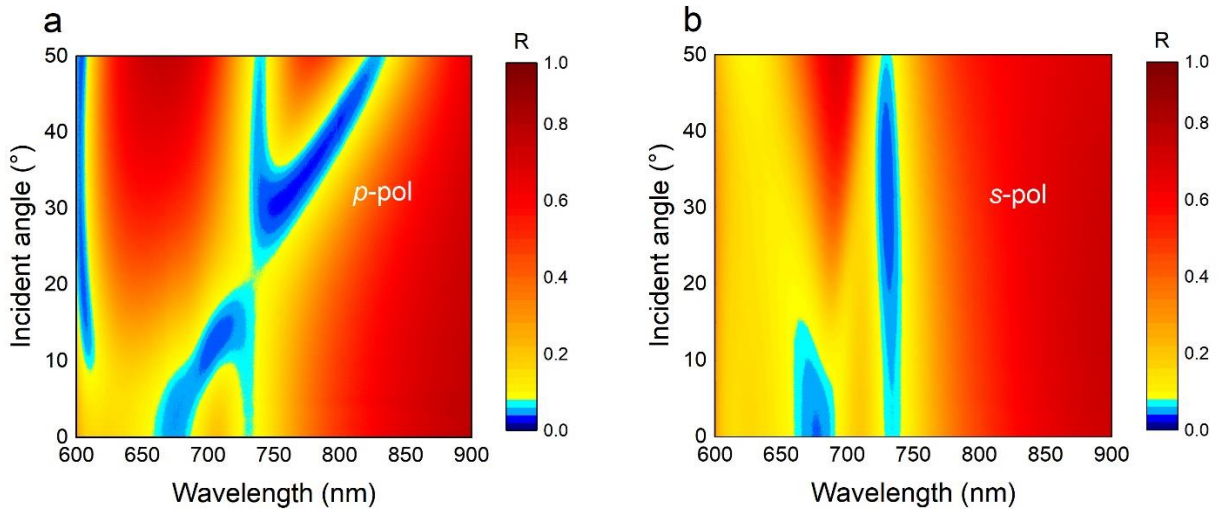

Figure S6. Reflection spectra of the regular array of Si nanopillars excited by using *p*- and *s*-polarized light. Angle-resolved reflection spectra measured for a regular array of Si nanopillars with p = 320 nm by using a) *p*- and b) *s*-polarized white light as the excitation source.

Supplementary Note 7: Procedure for fabricating Si nanopillars on an Au/SiO_2 substrate

In this work, we fabricated regular arrays of Si nanopillars with large (p = 5.0 μm) and small (p ~ 300 nm) periods by using the combination of electron beam lithography and reactive ion etching. A detail description of the fabrication process has been provided in the Methods of the main text. In Figure S7, we present the flow chat illustrating the fabrication process of regular arrays of Si nanopillars.

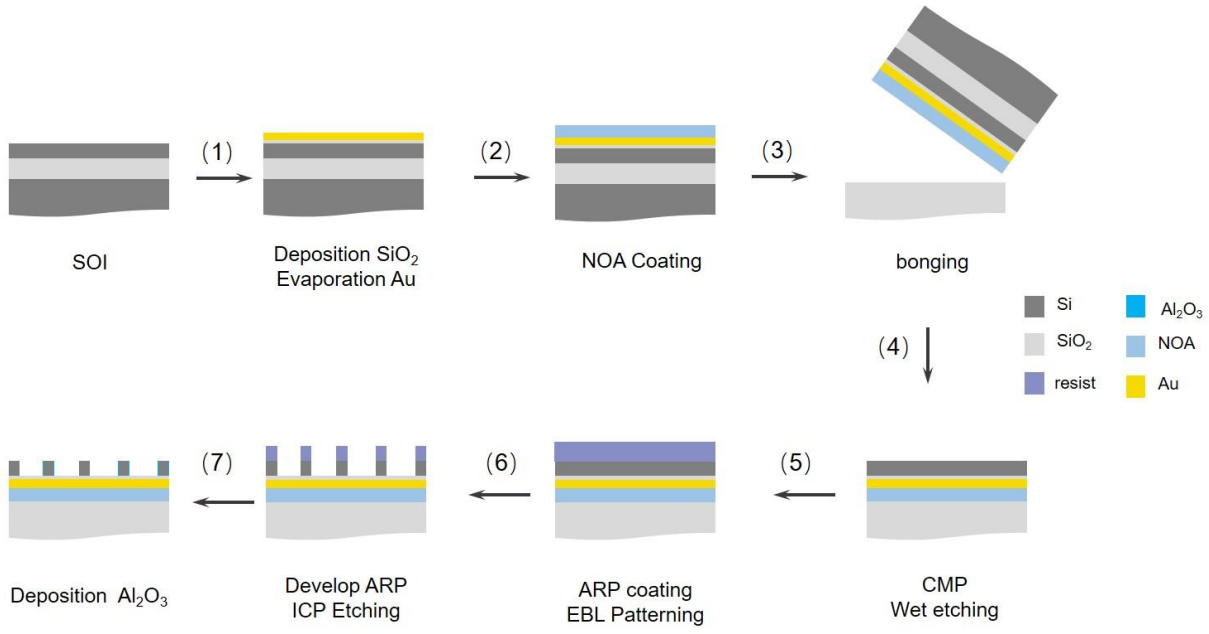

Figure S7. Procedure for fabricating Si nanopillars on an Au/SiO_2 substrate. Flow chat for the fabrication of Si nanopillars. (1) Silicon-on-insulator (SOI) wafer (SOITEC) used for the fabrication of Si nanopillars. It consists of a 725-μm -thick undoped <100> Si substrate, a 2-μm-thick SiO_2 middle layer, and a 220-nm-thick crystalline-silicon (c-Si) top layer. A 100-nm-thick gold (Au) film and a 10-nm-thick silica (SiO_2) film were deposited sequentially on the SOI wafer. (2) A UV light curable adhesive (NOA61) was spin-coated on the sample. (3) The sample was bonded to a quartz substrate and illuminated by using 365-nm ultraviolet LED light to cross-link

the adhesive for four hours. In order to achieve optimum adhesion, the sample was beforehand baked at 50°C for one day. (4) The Si substrate was then removed by chemical polishing and dry etching. A c-Si on quartz substrate was obtained by removing the SiO_2 substrate of the SOI wafer with hydrofluoric (HF) acid. (5) A positive resist (ARP6200.09) was coated directly onto the c-Si at 4000 RPM for 60 seconds and baked on a hotplate at 180°C for 10 minutes. (6) The pattern was exposed by using an electron-beam lithography system (EBPG5000Plus, Raith) operated at 100 kV. The resist was developed with xylene and the pattern transfer was realized by using an inductively coupled plasma tool (Oxford Instruments). (7) The fabricated Si nanopillars were covered with 5-nm-thick Al_2O_3 layer by using an atomic layer deposition system (SUNALE R-150, Picosun).

Supplementary Note 8: Morphology characterization of Si nanopillars

We fabricated regular arrays of Si nanopillars with different periods ranging from p = 300 nm to p = 700 nm. The size of each array was set to be 200 × 200 μm^2. The images of these regular arrays under a microscope are shown in Figure S8a. It can be seen that the regular arrays with different periods exhibited different colors under the illumination of white light. In Figure S8b, c, we show the SEM images (incline view) of two regular arrays of Si nanopillars with different periods (p = 300 nm and p = 600 nm). In Figure S8d–f, we present the SEM images (top view) of three regular arrays of Si nanopillars with different periods (p = 300, 500 and 700 nm).

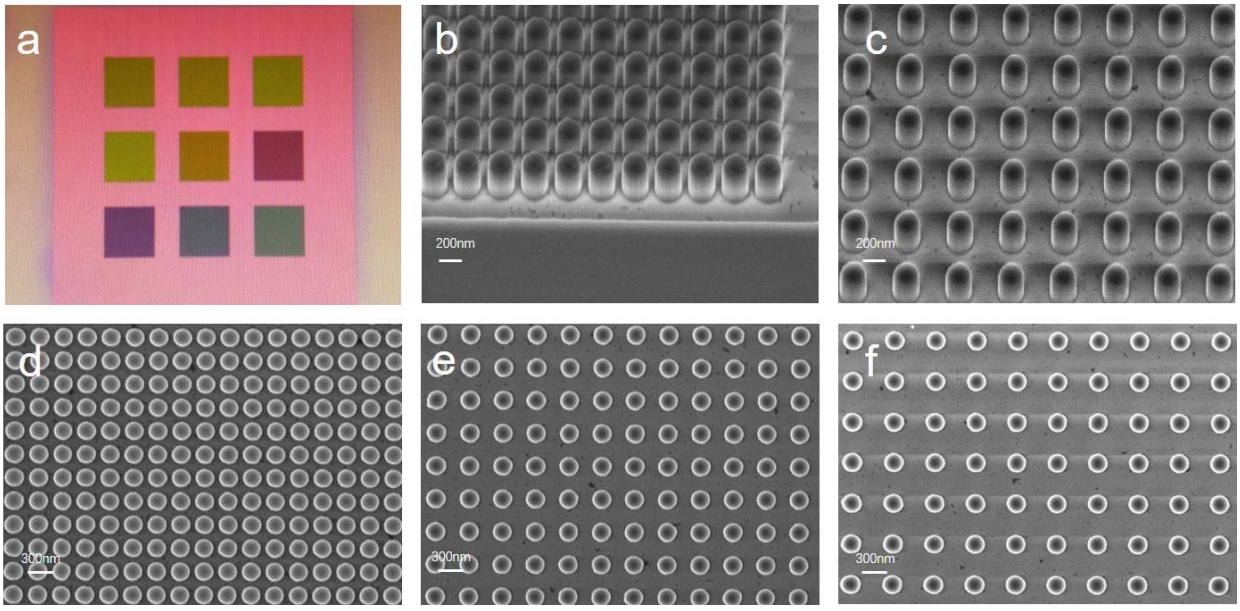

Figure S8. Morphology characterization of Si nanopillars. (a) Microscopic images of regular arrays of Si nanopillars with different periods ranging from p = 300 nm to p = 700 nm. (b,c) SEM images (incline view) of two regular arrays of Si nanopillars with different periods (p =300 nm and p = 600 nm). (d–f) SEM images (top view) of three regular arrays of Si nanopillars with different periods (p = 300, 500 and 700 nm).

Supplementary Note 9: Experimental setup used for the optical characterization

In Figure S9, we present a schematic for the experimental setup used to characterize the nonlinear optical responses of isolated and coupled Si nanopillars. A detailed description for the optical characterizations of the fabricated samples has been provided in the Methods of the main text.

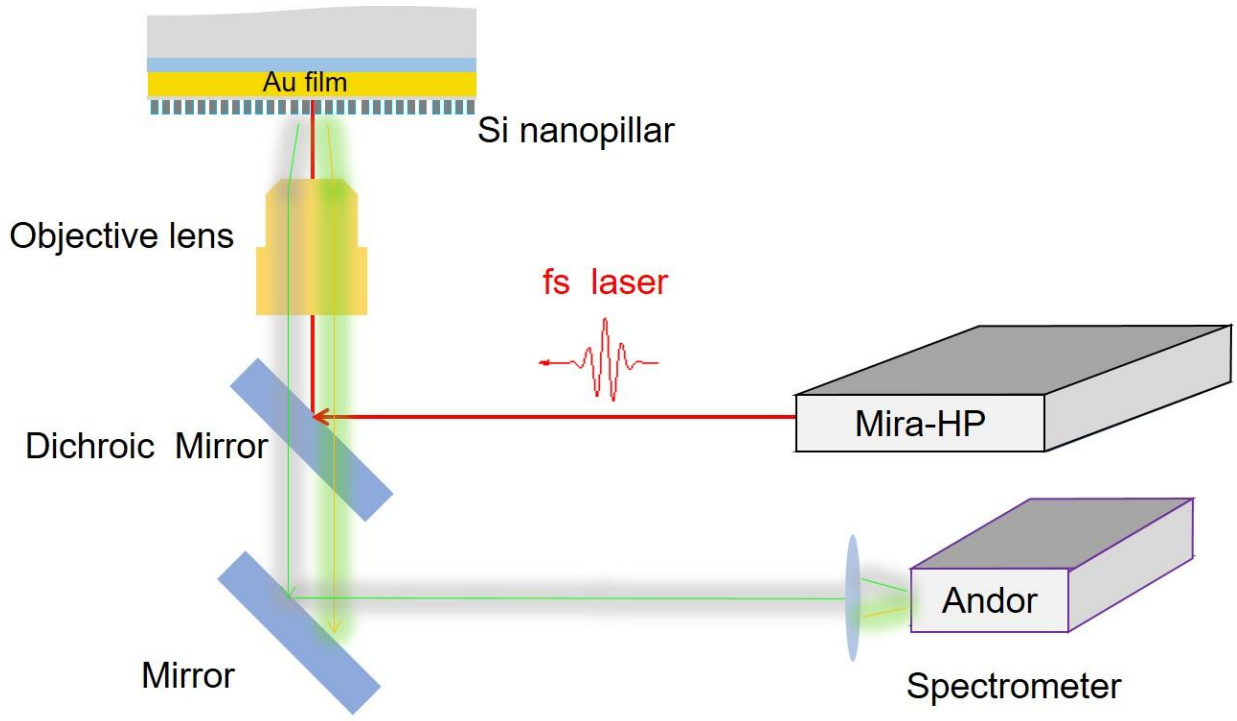

Figure S9. Experimental setup used to characterize the nonlinear optical responses of isolated and coupled Si nanopillars.

References

(1) Huang, Y.-W.; Chen, W. T.; Wu, P. C.; Fedotov, V.; Savinov, V.; Ho, Y. Z.; Chau, Y.-F.; Zheludev, N. I.; Tsai, D. P., Design of plasmonic toroidal metamaterials at optical frequencies. *Opt. Exp.* **2011,** *20* (2), 158993.

(2) Papasimakis, N.; Fedotov, V. A.; Savinov, V.; Raybould, T. A.; Zheludev, N. I., Electromagnetic toroidal excitations in matter and free space. *Nat Mater* **2016,** *15* (3), 263−271.

(3) Terekhov, P. D.; Baryshnikova, K. V.; Artemyev, Y. A.; Karabchevsky, A.; Shalin, A. S.; Evlyukhin, A. B., Multipolar response of nonspherical silicon nanoparticles in the visible and near-infrared spectral ranges. *Physical Review B* **2017,** *96* (3).